Proceedings of the 24th INTERNATIONAL CONGRESS on
Condition Monitoring and Diagnostics Engineering Management
Clarion Hotel Stavanger, Stavanger, Norway, 30th May – 1st June, 2011
(Editors) Maneesh Singh, Raj B. K. N. Rao and J. P. Liyanage,
COMADEM International, U.K., ISBN: 0-9541307-2-3

Motor Current Signature Analysis of a Variable Speed Drive for Motor Fault Diagnosis

Ahmed ALWODAI, Fengshou GU, Andrew BALL

University of Huddersfield, Queensgate, Huddersfield HD1 3DH, UK

ABSTRACT

The induction motor is one of the most used electric machines in the industry because of its strong and simplicity. This paper investigates the performance of conventional techniques such as sideband analysis in detecting broken rotor bars when the motor is fed from a common pulse width modulation voltage source inverter PWM-VSI drive for variable speed drives. The phase current signals are obtained under both the slip compensation mode and non-compensation mode. The spectra are compared between the healthy and faulty motors in the frequency domain. For the non-slip compensation, it has shown clear sidebands of the twice slip frequency which allows the detection of the broken bar and hence rotor faults under different speeds and higher loads. However, for slip compensation, the sideband pattern does not exist anymore and hence new features have to be investigated for fault detection when motors operate under these operating modes.

Keywords: Induction motor, voltage source inverter, motor current signature analysis (MCSA).

1. INTRODUCTION

The three-phase induction motor is the most commonly used type of motor in industrial applications because of its low maintenance needs and reliability. There are many types of induction motor designated according to their physical configuration, for example, squirrel-cage designs and wound rotor types. Squirrel-cage motors are most commonly used because of their simplicity.

There are several common modes of failure for an induction motor. As shown in Figure 1, the most common faults of induction motors can generally be classified as electrical and mechanical faults. The electrical faults can be either stator or rotor faults.

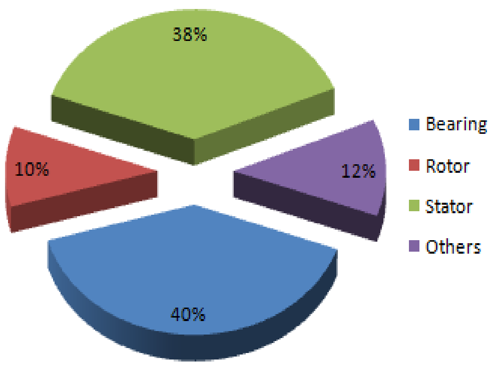

FIGURE 1. Induction machine faults

Stator faults include insulation break-down caused by mechanical vibration, heat, age, damage during installation, etc. Rotor bar faults can occur because of the different stresses that work on the rotor. Failures of induction motors cost time and money, making the use of an appropriate fault detection system, an attractive proposition.

To achieve variable speed, an induction motor is supplied by an inverter based on IGBT (Insulated Gate Bipolar Transistor) technology, which is fed by pulse width modulation from a voltage source inverter (PWM-VSI). PWM-VSI induction motors are usually more reliable than those operated directly online (Oumaamar et al., 2006).

Variable frequency drives with slip compensation produce reasonable accuracy in speed senseless control down to 100 rpm and are sufficient for low dynamics applications (Reljic et al., 2006). Slip compensation is used in AC drives to reduce the effect of motor slip. This paper presents the phase current signals of a healthy motor and one with a broken rotor bar, both with and without slip compensation. Motor current signature analysis is the fault detection technique which will be used.

2. AC VARIABLE FREQUENCY DRIVES

Variable frequency Voltage Source Inverters (VSI's) are widely used to control the speed of 3-phase squirrel cage induction motors and they do this by varying the stator frequency.

Variable frequency drives are used for two main reasons:

- To improve the efficiency of motor-driven equipment by matching speed to changing load requirements.
- To allow accurate and continuous process control over a wide range of speeds.

2.1 Structure of Variable Frequency Drives

The AC variable frequency drive consists of three main components as shown in Figure 2.

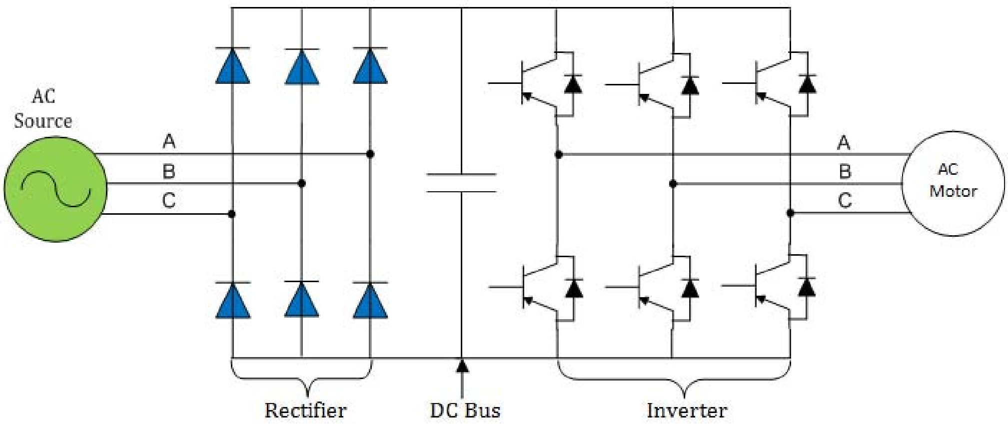

FIGURE 2. Principle of Variable Frequency Drive

- **Rectifier:**

The rectifier is connected to the supply network and generates a DC voltage supply which feeds the main DC link elements. The mains rectifier consists of a bridge circuit which converts the supply network from AC to DC. The DC voltage resulting from this always corresponds to the peak value of the connected mains voltage.

Where

$$V_{peak} = \sqrt{2}\ V_{rms} \tag{1}$$

Rectifiers can use diodes, silicon controlled rectifiers (SCR), or transistors to rectify power. Diodes are the simplest device and allow power to flow any time when the voltage of the proper polarity is present.

- **DC Bus:**

After the power flows through the rectifiers it is stored on a DC bus. The DC bus contains capacitors to accept power from the rectifier, store it, and later deliver that power through the inverter section. The DC bus may also contain inductors, DC links, chokes, or similar items that add inductance, thus smoothing the incoming power supply to the DC bus.

- **Inverter**

The last part of the VFD is an inverter. The inverter contains transistors that distribute power to the motor. The Insulated Gate Bipolar Transistor (IGBT) is a common option in modern VFDs. The IGBT can switch on and off several thousand times per second and accurately control the power sent to the motor. The IGBT uses a method named pulse width modulation (PWM) to provide a current sine wave of the desired frequency to the motor.

2.2 Operating Modes of VFD

A VFD system can operate under three basic modes: open-loop, slip compensation and closed-loop. Under both the slip compensation and closed-loop modes, the motor can run at the required speed accurately whereas under the open-loop, the speed of the motor reduces as load increases due to the slip effect of induction machines. The slip is usually about 0.03 at rated frequency, resulting in an effect which can be neglected in many applications (Munoz-Garcıa et al., 1998).

For variable-frequency operation, however, the slip for constant torque varies inversely proportional to the frequency. When the frequency decreases, the slip becomes significantly large and it can no longer be ignored. At very low frequencies this effect becomes so important that if not sufficiently compensated for the motor will not be capable to provide the load torque and will stop.

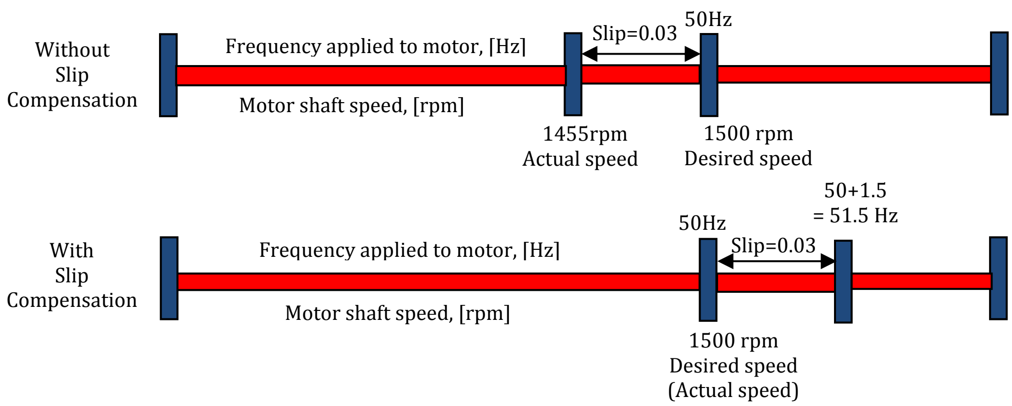

FIGURE 3. Slip Frequency Compensation

Figure 3 shows a function that needs the motor to provide full torque at 1500 RPM. The top part of the figure illustrates what occurs without slip compensation. The applied frequency is 50Hz, but the motor actual shaft RPM, due to slip, has a value of 1455.

The bottom part of Figure 3 illustrates how slip compensation automatically compensates for this condition by applying 1.5Hz of additional output frequency to the existing output frequency of 50Hz, resulting in a new output frequency of 51.5Hz. The motor shaft still slips back, but now the actual shaft speed is the desired 1500rpm.

2.3 Benefits of Variable Frequency Drives

According to (Carrier, 2005) variable frequency drives offer the following benefits:

- simple installation
- low motor starting current
- high power factor
- energy savings
- lower kVA
- reduction of thermal and mechanical stresses on the motor during starts

3. MOTOR CURRENT SIGNATURE ANALYSIS

Motor current signature analysis (MCSA) is an increasingly commonly used fault detection method. This technique depends upon locating (by spectrum analysis) specific harmonic components in the line current produced by rotating flux components caused by faults, for instance, broken rotor bars and shorted turns in stator windings (Verucchi et al.,2008; Thomson,2001) . As a result, this method can detect these faults at an early stage and consequently avoid complete failure of the motor. In addition, it does not need the installation of a measurement system and it can be used online.

The operation of a three phase induction motor is based on Faraday's law. When AC current passes through stator windings which are displaced by an electrical phase difference of 120˚, a magnetic field is created with a rational speed known as the synchronous speed which is given by this formula:

$$N_s = \frac{120 f_s}{p} \quad (2)$$

Where

N_s=synchronous speed in rpm

f_s= supply frequency

p=number of poles per phase

The rotor of the induction motor always rotates at a speed (N_r) which is less than the synchronous speed, and the difference between synchronous speed and rotor speed is called slip speed (N), which can be expressed as follows.

$$N = N_s - N_r \quad (3)$$

The slip can be expressed in per unit terms by the flowing formula:

$$s = \frac{N_s - N_r}{N_s} \quad (4)$$

The rotor speed never reaches the synchronous speed, actually if the rotor did turn at the same rate as the synchronous speed the flux will not cut the rotor bars and the induced voltage and resulting current will be zero. Under the normal operation condition the slip is between 3% and 10% at full load for squirrel cage induction motors (Fitzgerald et al., 1986).

With broken rotor bars in the motor there is an additional backward rotating magnetic field produced, which is rotating at the slip speed with respect to the rotor. This rotating magnetic field can be given by

$$N_b = N_r - N = N_s(1 - s) - s\,N_s = N_s(1 - 2s) \quad (5)$$

Equation (5) can be rewritten in terms of frequency:

$$f_b = f_s(1 - 2s) \quad (6)$$

This means that the frequency f_b is a twice slip frequency component spaced $2sf_s$ down from f_s. . This lower sideband is due to broken rotor bar, while there is an upper sideband at $2sf_s$ above f_s which is induced by the oscillations of torque and speed at $2sf_s$.

The twice slip frequency sidebands that occur around the supply frequency can be given by

$$f_b = f_s(1 \pm 2s) \quad (7)$$

According to several researchers, broken bars actually give rise to a sequence of such sidebands given by (Loránd et al., 2004):

$$f_b = f_s(1 \pm 2ks) \quad (8)$$

Where: k=1, 2, 3,...

The rotor fault of an induction motor can be clearly indicated by appearance in the spectrum of sidebands given by Equation (8).

4. EXPERIMENTAL SET UP

Figure 4 shows a schematic of the test rig which was used in the experiment. The test rig consists of four sub-systems, namely, the driving motor, the load, the measuring devices and the data acquisition system.

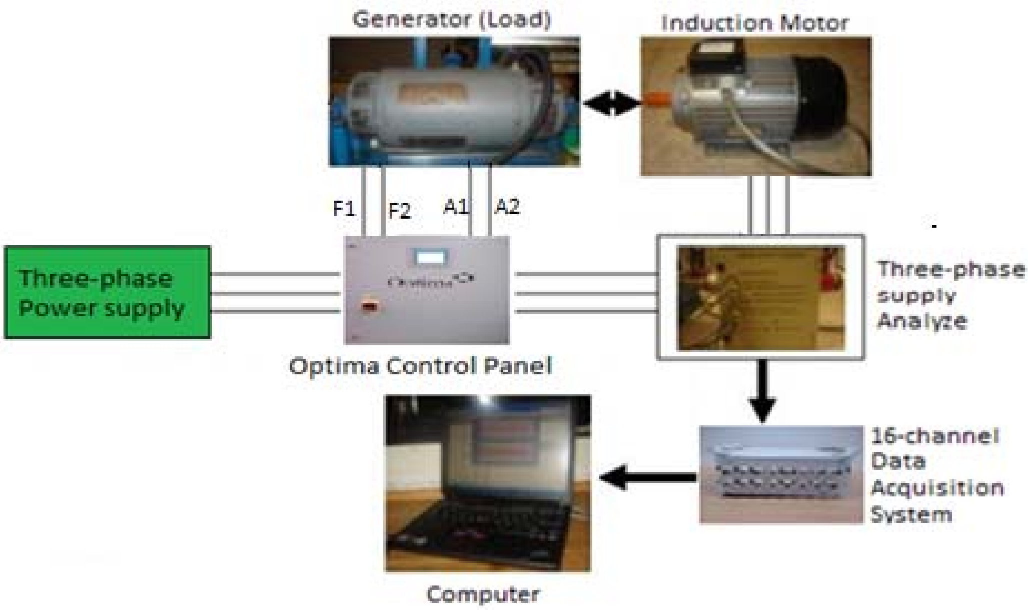

FIGURE 4. Schematic of the experimental setup

The driving motor is a 4kW three-phase 4-pole induction motor. The rotor is a die-cast aluminum squirrel cage with 28 skewed bars. These bars are of a deep design to provide a high starting torque from a low starting current (Hughes, 2001).

The induction motor is directly coupled with a loading DC generator. The field of the generator is connected to DC source by wires F_1 and F_2 while output power is transmitted by wires A_1 and A_2 (see Figure 4).The generator was supported by outer casing bearings so that the torque applied to the stator can be measured. The generated power was fed back to the mains electrical grid and the load in the induction motor can be adjusted by changing the field resistance of the DC generator. The operating load can be varied from no load to full load via the control panel. The power supply measurement box was designed to measure motor voltages, currents and power, using Hall Effect voltage and current transducers and a universal power cell.

During the experimental work all the collected data was acquired using a GST YE6232B data acquisition system. This system has 16 channels, each channel with a 24 bit analogue-digital converter with a maximum sampling frequency of 96 kHz.

The tested three-phase squirrel cage induction motor has the following data: 5.5 HP (4 kW), 230/400 V (Δ/Y), 15.9/9.2 A (Δ/Y) and 1420 rpm.

Tests were carried out for four different loads with the healthy motor, and with a similar motor having a full broken rotor bar. The rotor fault was simulated by interrupting the rotor bar by drilling into the rotor as can be seen in Figure 5.

FIGURE 5. Squirrel cage rotor with full broken bar

The measured phase current signal was analysed by using the Fast Fourier Transformation (FFT). The results obtained for the healthy motor and broken rotor bar motor were compared, particularly looking for sideband components having the frequencies given by equation (8).

5. EXPERIMENTAL RESULTS

5.1 Detection under non-slip compensation

As can be seen from figures 6, 7, 8 and 9, the detection of the slip frequency sidebands at no-load (and also at low loads) is too difficult, since the current in the rotor bars is small. The most revealing results were obtained at high loads, especially near to the rated load.

Figure 6 shows phase current spectra under four different load conditions at 50% speed. The applied frequency is 25 Hz (synchronous speed=750 rpm). As the load increases the motor speed decreases, with motor speeds under healthy motor conditions of 749, 739, 727and 714rpm. At zero, 25%, 50% and 75% load, respectively.

Figures 6, 7 and 8 illustrate phase current spectra under different loads and at speeds of 50%, 75%, and 100% rated speed. As can be seen from the figures, as the frequency decreases, the slip becomes larger. With the motor speed at 50% (applied frequency 25.1 Hz) and the motor operated at 75% load, the slip was 0.048, however the slip was 0.041 under 75% load and at 75% speed.

5.2 Detection under slip compensation

The slip compensation technique of speed control does not monitor the actual shaft speed for speed adjustment, rather it uses drive output current transducers to monitor the current drawn by the motor and alters the main frequency so that the motor speed can maintain desired speed as steady as possible. However, because of inevitable load fluctuations the main supply frequency realized in this way will have some fluctuations accordingly, or it not as stable as that without slip compensation.

Figure 9 shows phase current spectra under different loads at 100% rated speed with slip compensation for healthy and broken rotor bar conditions. The computed values of lower sideband frequencies under broken bar conditions were 47.41, 47, 46.38 and 45.73 Hz, while the upper sideband frequencies were 51.7895, 53.20, 55.02, and 56.67 Hz, under zero, 25%, 50% and 75% rated load, respectively.

It is clear from the figure that the speeds are near consistent at different loads. For example the motor shaft speeds were 1455 rpm and 1454 rpm at zero and 75% rated load, respectively. These results show the advantage of a variable frequency drive with slip compensation.

On the other hand the current spectrum cannot show sidebands when using slip compensation. This is because of the harmonics that appear in current spectrum. To avoid this problem another technique has to be investigated.

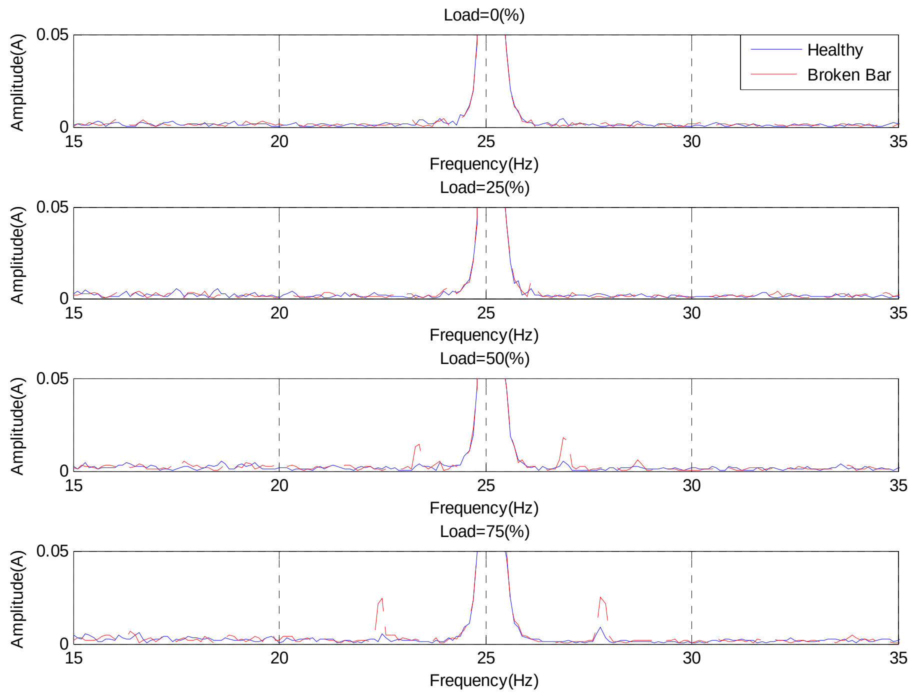

FIGURE 6. Phase current spectrum at 50% speed and with non-slip compensation

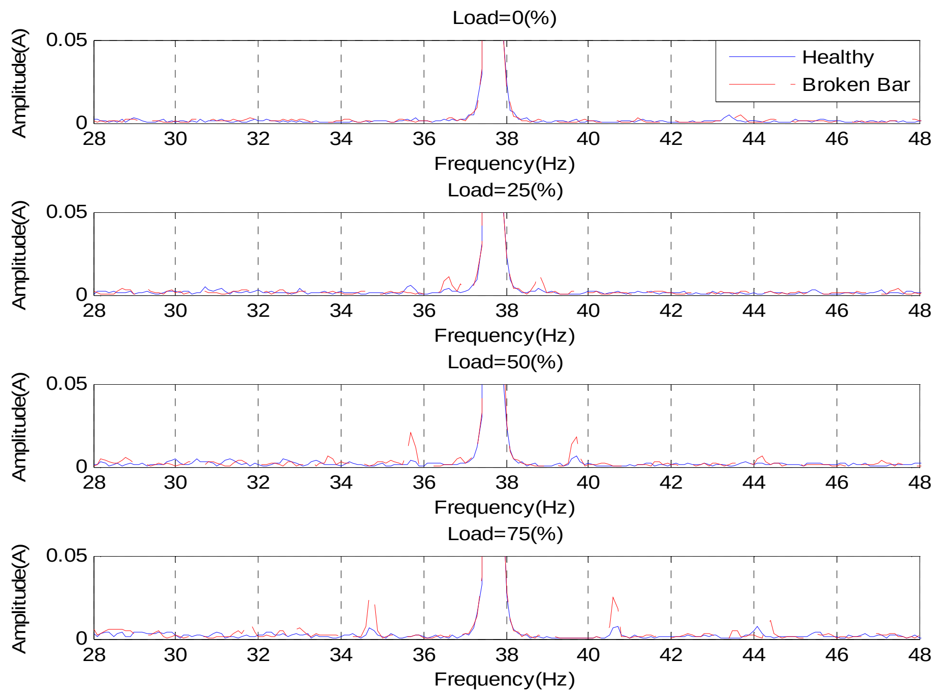

FIGURE 7. Phase current spectrum at 75% speed and with non-slip compensation

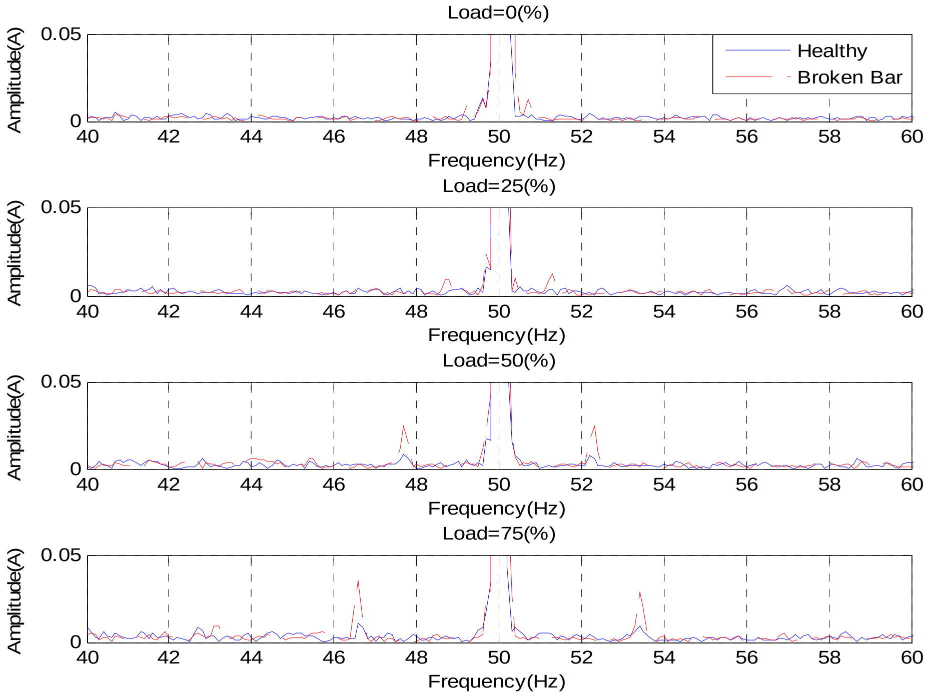

FIGURE 8. Phase current spectrum at 100% speed and with non-slip compensation

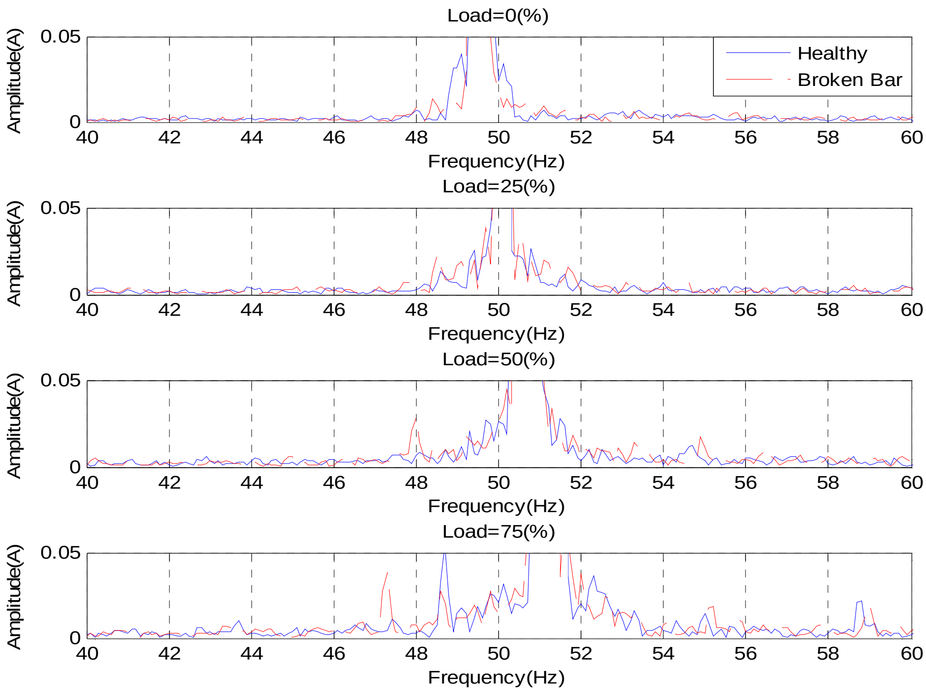

FIGURE 9. Phase current spectrum under healthy and broken bar condition with slip compensation

6. CONCLUSIONS

A variable frequency drive is studied under both slip compensation and non-slip compensation operating modes to verify spectrum based motor fault detection techniques. In particular, the twice slip frequency sidebands are investigated for broken bar detection. Experimental results show that for non-slip compensation operation MCSA retains its detection and diagnosis capability at different motor speeds but only for operating loads above 50% because the recognition of the slip frequency sidebands is not easy at lower loads.

For the slip compensation operation it is not clear that the spectra under different loads have the sideband pattern, meaning that traditional MCSA techniques are not suitable for detecting the broken bar faults in these circumstances and hence new approaches have to be investigated.

REFERENCES

Oumaamar, M.E., Babaa, F., Khezzar, A. and Boucherma, M. 2006. Diagnostics of Broken Rotor Bars in Induction Machines Using the Neutral Voltage., Proceedings of ICEM'96, Chania, Greece, 2-5 Sept. 2006.

Reljic, D., Ostojic, D. and Vasic, V. 2006. Simple Speed Sensorless Control of Induction Motor Drive. Sixth International Symposium Nikola Tesla. Belgrade, Serbia, October 18 – 20, 2006

Fitzgerald, A.E., Charles, K. J. and Umans, S. D. 1986 Electric Machinery 4th Edition McGraw-Hill Book Company Co- Siggapore, ISBN 0-07-Y66279-7,pp. 409-420.

Loránd, S., Barna, D.J. and Ágoston, B.K. 2004. Rotor Faults Detection in Squirrel-Cage Induction Motors by Current Signature Analysis. IEEE-TTTC - International Conference on Automation, Quality and Testing, Robotics. Cluj-Napoca, Romania, May 13 – 15, 2004

Carrier. 2005. Variable Frequency Drive: Operation and Application Of Variable Frequency Drive (VFD). Technology Carrier Corporation Syracuse, New York, October 2005.

Hughes, A. 2001. Electric Motors and Drives-fundamentals, Types and Applications. *Newnes*, 0750617411s

Verucchi, C.J., Acosta G.G. and BENGER F.A. 2008. A Review on Fault Diagnosis of Induction Machines. Latin American Applied Research, 38, pp.113-121

Thomson, W. T. 2001. On-line MCSA to Diagnose Shorted Turns in Low Voltage Stator Windings of Three phase Induction Motors Prior to Failure. IEEE International Conference on Electric Machines and Drives, pp 891-898.

Munoz-Garcıa, A., Lipo, T. A. and Novotny, D. W. 1998. A New Induction Motor *V/f* Control Method Capable of High Performance Regulation at Low Speeds. IEEE Transactions on Industry Application, Vol. 34, No. 4, pp. 813-821